Sample self-stacking in zone electrophoresis

Theoretical description of the zone electrophoretic separation of minor compounds in the presence of bulk amounts of a sample component with high mobility and like charge

Petr Gebauer

Institute of Analytical Chemistry, Czechoslovak Academy of Sciences, Veveři 97, CS-611 42 Brno (Czechoslovakia)

Wolfgang Thormann

Institute of Clinical Pharmacology, University of Berne, Murtenstrasse 35, CH-3010 Berne (Switzerland)

Petr Boček

Institute of Analytical Chemistry, Czechoslovak Academy of Sciences, Veveři 97, CS-611 42 Brno (Czechoslovakia)

ABSTRACT

A theoretical description of the sample self-stacking effect in zone electrophoresis is given. This effect applies to samples that contain a high concentration of an ionic component with high mobility and like charge. After current application, the sample components are stacked at the rear of the zone of the major component by an isotachophoretic mechanism. Later, the sample substances gradually destack in order of increasing mobility and continue to migrate and separate by the normal mechanism of zone electrophoresis. Simple relationships are derived for model systems allowing an explicit description of the properties of such systems and the zone parameters such as detection time, variance and resolution. The reliability of the model presented is verified and illustrated by computer simulation of selected examples. It is shown that the described sample self-stacking effect provides at least the same concentrating power as is obtained with conventional zone electrophoretic sample stacking.

INTRODUCTION

In principle, zone electrophoresis is a dispersive technique. Once introduced into the column and migrating in the background electrolyte (BGE), the sample zone broadens by diffusion and other dis-

persive effects. One of the most important problems with this technique is therefore the question of how to make the starting sample peak as sharp as possible to get narrow and well separated peaks into the detector. There are various approaches that are employed to achieve this aim. In the sample stacking technique [1,2], a large zone of diluted sample (sample dissolved in water or diluted BGE) is introduced into the column by hydrodynamic flow. During the electrophoresis run, the sample compo-

---

Correspondence to: Dr. P. Gebauer, Institute of Analytical Chemistry, Czechoslovak Academy of Sciences, Veveři 97, CS-611 42 Brno, Czechoslovakia.

nents are concentrated when passing the sample/ BGE interface and the size of the sample zone is thus considerably reduced. The field amplification technique [3] is based on the same principle, the difference being that the diluted sample solution is applied by the effect of an electric field. When a suitable slow ion is added to the sample, its stacking by an isotachophoretic mechanism temporally proceeds [4]. A very effective tool is the on-line combination of isotachophoresis and capillary zone electrophoresis [5–8]. In the first (isotachophoretic) step, concentration of the sample components into narrow, consecutive zones is achieved. These zones are introduced in the second step into a zone electrophoretic system where they are separated. This technique, however, requires special instrumentation and cannot be run on commercial instruments for capillary zone electrophoresis.

An important factor affecting zone electrophoretic separation is the composition of the sample solution; this was demonstrated by computer simulation [9,10]. Problems may occur when analysing samples that contain one component in large excess. A typical example is body fluid involving large amounts of sodium and chloride ions. When looking for components that are present in minor concentrations only, further dilution of the sample for using the above-mentioned techniques may not be advantageous and will not bring an improvement. Fortunately, the ion that is in excess usually has a high mobility. As was shown previously [11–13], this causes a temporal stacking of the minor sample components at the rear of the sample zone, thus permitting their separation as narrow zones. It is the aim of this paper to present a simple theoretical description of this type of system. The reliability of the model presented is verified and illustrated by computer simulation.

THEORETICAL

For the theoretical treatment of the present problem, a very simple zone electrophoretic system had to be selected as a model to be able to provide a sufficiently explicit description. The background electrolyte consists of a solution of anion B^- of a strong acid HB and of cation RH^+ of a weak base R. The BGE is considered to be in the buffering optimum of the weak base where $C_R = 2c_{RH} = 2c_B$.

(C is the total and c the ionic concentration). The investigated sample contains a major concentration of a fast anion A^- of a strong acid HA and minor concentrations of anions X^- and Y^- of strong acids HX and HY, respectively, which are negligible when compared with the concentration of the major component. The concentrations of the minor sample components are assumed to be negligible even when being concentrated and stacked during the electrophoretic separation process. The sample solution is assumed to have the same pH as the background electrolyte (although this changes during the electrophoresis, the maximum pH deviation will not be greater than 0.2 pH units). As all investigated sample components are strong anions, the influence of small pH differences on their migration behaviour can be neglected. By this approach the changes in the concentrations of both H^+ and R along the column are neglected. Moreover, the pH is assumed to lie within the neutral region where the contribution of H^+ to conductivity can also be neglected.

We further assume that we have a hydrodynamically closed capillary system with absence of hydrodynamic and electroosmotic flow, and are operating with constant electric current. The amount of sample substance A introduced is so high that, under the given operating conditions, electromigration is the major dispersion effect and other than diffusional dispersions can be neglected anywhere except the regions of self-sharpening boundaries. The mobilities of the anionic species are selected so that $u_A > u_X > u_Y > u_B$. This is an important prerequisite for proper functioning of the discussed type of systems: the major sample component must have the highest mobility to act as the stacking leader and the background co-ion must have the lowest mobility to act as the stacking terminator.

Migration of the major sample component

Before discussing the behaviour of the minor sample components in the given system, the characteristics of the evolution of the concentration profile of the major sample substance A must be briefly given. We assume that the sample is introduced hydrodynamically into the (one-dimensional) column as a rectangular concentration pulse (see Fig. 1a). The BGE and the sample are denoted zones 1 and 3, respectively. Let us put the origin of the x-axis ($x = 0$) into the right boundary between
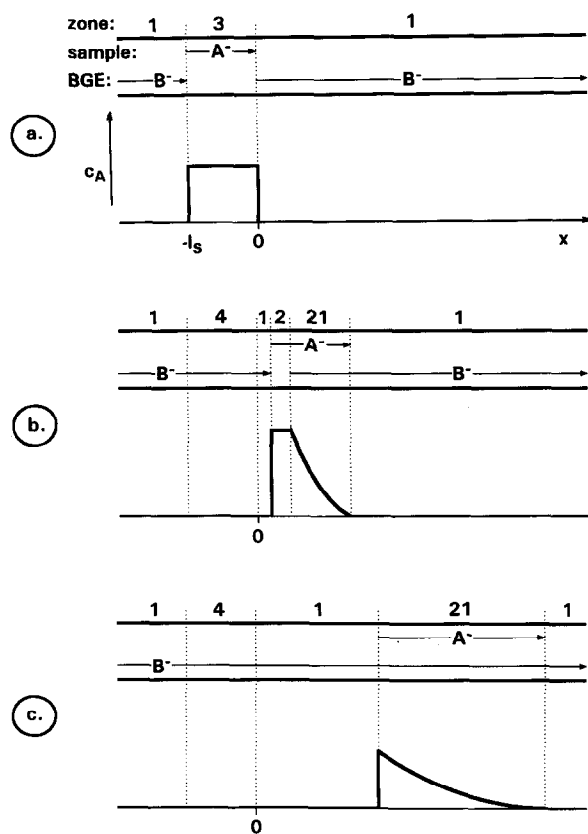
Fig. 1. Scheme of migration of a zone of anion A^- in the background electrolyte R^+A^- at three different values of electrophoresis time. (a) Initial state showing the position and designation of the zones (above) and concentration profile of the zone of A^-, being here a rectangular pulse of length l_S. (b) Situation after the entire zone of A^- has migrated through the point $x = 0$; the concentration profile consists of two distinguished parts, viz., a rectangular (isotachophoretic) one and a descending (transition or diffuse) one. (c) Situation where the zone of A^- is represented only by the diffuse descending concentration profile.

the sample zone and the background electrolyte (boundary 3–1), i.e., at the beginning of the separation compartment. Let l_S be the length of the original sample zone (length of the sampling compartment, see Fig. 1a).

When now passing electric current through the system so that anions move to the right, the zone of substance A migrates through the boundary 3–1 and readjusts its concentration isotachophoretically [14] to the conditions of zone 1. The so-formed zone of

substance A is denoted zone 2 (see Fig. 1b) and its readjusted concentration is given by

$$c_{A,2} = c_{B,1} \, m_B/m_A \tag{1}$$

where $c_{i,j}$ is the concentration of ion i in zone j, $m_i = (u_i + u_R)/u_i$ and u_i is the electrophoretic mobility of ion i.

The content of the sampling compartment is displaced by the BGE adjusted to the parameters of zone 3 (zone 4) and at the positions of the original sample boundaries (1–3 and 3–1), the stationary concentration boundaries 1–4 and 4–1 are found. During the process when the sample zone migrates out of the sampling compartment, its rear boundary remains sharp (boundary 4–3 between the sample zone 3 and the BGE zone 4 adjusted to its parameters); it moves with the velocity

$$v_{4-3} = i \, u_A/\kappa_3 = i \, u_B/\kappa_4 \tag{2}$$

where i is the electric current density and κ_3, e.g., is the specific conductivity of the sample solution given by

$$\kappa_3 = F \, c_{A,3}(u_A + u_R) \tag{3}$$

where F is the Faraday constant. The rear boundary of the sample zone reaches the point $x = 0$ at the time

$$t_0 = l_S/v_{4-3} = l_S \, \kappa_3/i \, u_A \tag{4}$$

It then continues to migrate as a sharp boundary but now between zones 1 and 2 (boundary 12, see Fig. 1b) with the velocity

$$v_{1-2} = i \, u_A/\kappa_2 = i \, u_B/\kappa_1 \tag{5}$$

Whereas the rear boundary of zone 2 migrates as an isotachophoretic (sharp) boundary, no self-sharpening effect will apply at its front. Here the originally rectangular concentration profile spreads into a more and more diffuse transition zone (zone 21, see Fig. 1b). The velocities of its front and rear edges correspond to velocities of single ions A^- and B^- in zones 1 and 2, respectively:

$$v_{A,1} = i \, u_A/\kappa_1 \tag{6}$$

$$v_{B,2} = i \, u_B/\kappa_2 \tag{7}$$

The time- and coordinate-dependent parameters of the transition zone 21 can be obtained by solving the set of partial differential equations (continuity equations valid for the three substances A, B and R).

The solution of such a system for three fully ionized species was given by Weber [15] (see also ref. 16). The present system brings a new aspect in that the counter-substance is a weak base. Fortunately, we may take advantage of the rule [17] that the total concentration of neutral particles remains constant with time; for the present system it holds in the form $\partial c_R/\partial t = 0$. Therefore, the continuity equation for the counter-substance can be written in the same form as for a fully ionized species and the set of continuity equations may be solved in the same way as referred to above.

For the descending concentration profile of substance A in zone 21 (see Fig. 1b), e.g., it holds that

$$c_{A,21} = \frac{u_B \, c_{B,1} m_B}{m_A(u_A - u_B)}\left[\left(v_{A,1} \cdot \frac{t}{x}\right)^{\frac{1}{2}} - 1\right] \qquad (8)$$

and for the conductivity we obtain

$$\kappa_{21} = F[c_{A,21}(u_A + u_R) + c_{B,21}(u_B + u_R)] = \\ \kappa_1(v_{A,1} \, t/x)^{\frac{1}{2}} \qquad (9)$$

The velocity of the rear boundary of zone 2 is higher than that of the rear edge of the transition zone 21, $v_{1-2} > v_{B,2}$; the boundary 1–2 and the edge 2–21 meet at the point x_d. The following balance holds:

$$x_d/v_{B,2} = t_0 + x_d/v_{1-2} \qquad (10)$$

from which we obtain

$$x_d = l_S \cdot \frac{\kappa_3}{\kappa_1} \cdot \frac{u_B}{u_A} \cdot \frac{u_B}{u_A - u_B} \qquad (11)$$

Note that all the time of its existence zone 2 has kept its isotachophoretic character and did not contain any amount of the background substance B (see Fig. 1b). The respective time of disappearance of zone 2 is then

$$t_d = x_d/v_{B,2} = l_S \, \kappa_3/i \, (u_A - u_B) \qquad (12)$$

Starting at this time point, the sample zone (zone of anion A^-) is formed only by the descending concentration profile as shown in Fig. 1c. Note that now the sample zone is completely mixed, i.e., substance A migrates completely on the background of anion B^-. Whereas the front edge of this zone 21 migrates still with constant velocity given by eqn. 6, its rear edge now consists of the sharp boundary 1–

21. The migration velocity of this boundary is a function of time [16] and may be written as

$$v_z = dx_z/dt = i \, u_A/\kappa_z \qquad (13)$$

where the subscript z relates to the parameters of zone 21 at its rear boundary 1–21. By expressing κ_z from eqn. 9, we obtain the differential equation

$$dx_z/dt = (v_{A,1} \, x_z/t)^{\frac{1}{2}} \qquad (14)$$

Integration (starting at x_d and t_d) provides the position of boundary 1–21 at any time $t > t_d$:

$$x_z^{\frac{1}{2}} = (v_{A,1}t)^{\frac{1}{2}} - x_d^{\frac{1}{2}} \cdot \frac{u_A - u_B}{u_B} \qquad (15)$$

Migration of a minor component

Let us now consider the same situation and system as described in the previous section with the one exception that the sample zone (zone 3) contains additionally a minor amount of the substance X (Fig. 2a). After application of electric current, both anions A^- and B^- behave in the same way as described in the previous section and only the presence of anion X^- makes a difference. An own (isotachophoretic) zone of X^- starts to be formed between the zones of A^- (zone 3 or 2 from Fig. 1, now including the minor content of X^-) and of B^- (zone 4 or 1 from Fig. 1). Let us describe the situation at a time point corresponding to Fig. 1b where the whole sample has left the sampling compartment. As is depicted in Fig. 2b, the ions of X^- leave zone 2 of the major sample substance A both via its rear boundary (to be stacked here, as it holds that both $v_{X,2} < v_{A,2}$ and $v_{X,1} > v_{B,1}$) and via its front edge (to penetrate into the diffuse part of the A^- zone, as it holds that $v_{X,2} > v_{B,2}$).

The stacking process proceeds by the isotachophoretic mechanism. As the isotachophoretic steady-state concentration of X^- in its own zone is independent of its concentration in the sample zone, it may be higher than the latter by many orders of magnitude [14]. This indicates an effective concentrating potential that applies even in our case when the substance X is present in such a minor amount that the sample zone does not reach the adjusted concentration plateau and, instead, forms only a small concentration peak behind the zone of A (Fig. 2b).
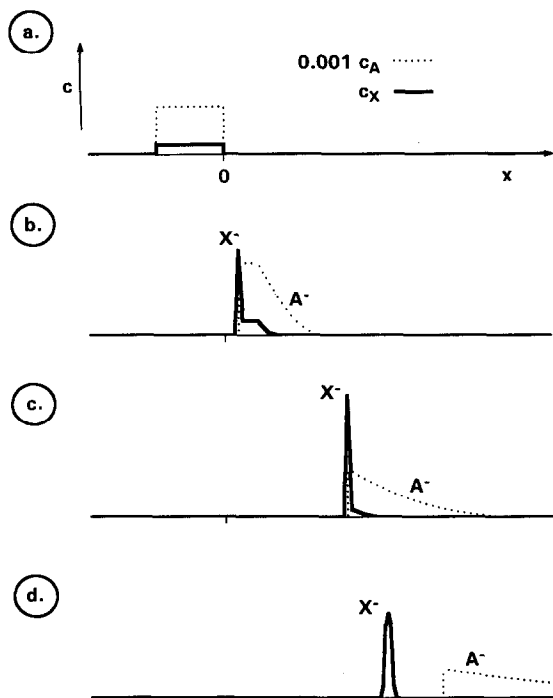
Fig. 2. Scheme of migration of a sample zone containing a major amount of a fast anion A^- and a minor amount of a slower anion X^-. (a) Initial state. (b) Starting phase of separation of both anions; in addition to the rectangular (isotachophoretic) part of the pattern where the concentration ratio still corresponds to the initial state, concentration (stacking) proceeds at the rear of the zone of A^- and, additionally, some penetration of X^- into the diffuse part of the zone of A^- is seen. (c) Situation where the stacking of X^- at the rear boundary of the A^- zone is almost complete; the amount of residual X^- in the diffuse A^- zone is already very small. (d) Complete separation and start of diffusional broadening of zone X.

The concentration of X^- having migrated forward into zone 21 is negligible in comparison with those of A^- and B^-; its migration behaviour is thus controlled by the parameters of zone 21 only as described in the previous section. Obviously X^- cannot reach the front edge of zone 21 as $u_X < u_A$; instead, it forms its own descending concentration profile with its own edge. As each point of zone 21 migrates with a constant velocity (in the present instance directly equal to x/t) [15,16], the migration velocity of the front edge of the X^- profile, $v_{X,m}$, must also be constant. The x/t point of zone 21 that corresponds to this velocity can be found from the equality

$$v_{X,m} = i\, u_X/\kappa_{21}(x/t) = x/t \tag{16}$$

By expressing κ_{21} by analogy with, e.g., eqn. 9, we obtain after rearrangement

$$v_{X,m} = \frac{i\, u_X}{\kappa_1}\, \frac{u_X}{u_A} \tag{17}$$

After zone 2 has disappeared from the system (i.e., at time points $t > t_d$, see eqn. 12), the process of separation of X from A continues but X^- now migrates out of zone 21 and is stacked at the 1–21 boundary (Fig. 2c). Note that the zone system still migrates in stack as both the 1–21 boundary keeps its self-sharpening properties and the migration velocity of X^- in (the rear) zone 1 given by

$$v_{X,1} = i\, u_X/\kappa_1 \tag{18}$$

is still higher than the migration velocity of the boundary itself ($v_{X,1} > v_z$). Of course, this boundary stack continuously speeds up with time as v_z increases (see eqn. 13).

The time point is now of interest when the sample zone leaves the stack. As is shown below, at this time point the migration velocity of X^- in zone 1 ($v_{X,1}$, eqn. 18) reaches the value of the migration velocity of the boundary itself (v_z, eqn. 13) and, simultaneously, the last traces of X^- migrate out of the transition zone 21. The time $t_{X,e}$ of equal migration velocities, $v_{X,1} = v_z$, can be obtained from eqn. 18 and 14 after substitution using eqns. 5–7, 12 and 15 and rearrangement:

$$t_{X,e} = t_d \cdot \frac{(u_A - u_B)^2}{(u_A - u_X)^2} \tag{19}$$

At that time, the rear boundary of zone 21 is at the point $x_{X,e}$ that is determined by eqn. 15 (with $x_z = x_{X,e}$ and $t = t_{X,e}$):

$$x_{X,e}^{\frac{1}{2}} = (v_{A,1}\, t_{X,e})^{\frac{1}{2}} - x_d^{\frac{1}{2}} \cdot \frac{u_A - u_B}{u_B} \tag{20}$$

By substitution and rearrangement using eqns. 19, 12, 5–7 and 17, we obtain the expression

$$x_{X,e} = t_d\, v_{A,1} \cdot \frac{(u_A - u_B)^2}{(u_A - u_X)^2} \cdot \frac{u_X^2}{u_A^2} = t_{X,e}\, v_{X,m} \tag{21}$$

which shows that the values of $x_{X,e}$ and $t_{X,e}$ also express the position of the front edge of X^- in zone 21 (see eqn. 12). In other words, the last ions of

substance X leave zone 21 just at the moment when the zones of X^- and A^- lose their immediate contact, *i.e.*, the zone of substance X^- starts to migrate out of the stack.

After the zone of substance X leaves the stack, it migrates in a normal zone electrophoretic mode in the BGE (in zone 1) (see Fig. 2d). Its position at a time point $t > t_{X,e}$ is given by the balance

$$x_{X,t} = x_{X,e} + (t - t_{X,e})v_{X,1} \tag{22}$$

Rearrangement using eqns. 18, 19 and 21 results in

$$x_{X,t} = v_{X,1} \left[t - t_d \cdot \frac{(u_A - u_B)^2}{(u_A - u_X)u_A} \right] \tag{23}$$

Detection time and variance of the zone of a minor component

On the basis of the above considerations, we are able to give explicit expressions of the zone parameters that are important for analytical practice. We assume that the detection of the zone of the minor sample component X proceeds after it has left the stack, *i.e.*, at times $t > t_{X,e}$. As will be shown below (see Results and Discussion), this approximation is justified.

For a detector placed at point x_r, we obtain for the detection (elution) time of zone X from eqn. 23 directly

$$t_{X,r} = \frac{x_r}{v_{X,1}} + t_d \cdot \frac{(u_A - u_B)^2}{(u_A - u_X)u_A}$$

$$= \frac{x_r}{v_{X,1}} + t_{X,e} \cdot \frac{u_A - u_X}{u_A} \tag{24}$$

The first term in this equation represents the expression for the normal zone electrophoretic mode of migration. The second term expresses the delay of zone X in the present system (when compared with normal zone electrophoresis) caused by the fact that the zone of substance X migrates a certain time in stack, *i.e.*, slower than corresponds to its zone electrophoretic velocity, $v_{X,1}$. Note that both t_d and $t_{X,e}$ are directly proportional to $c_{A,3}$ (see eqns. 12, 3 and 19).

For expressing the zone variance we assume that diffusion is the only dispersion effect that applies. While migrating in stack, the zone of X is very sharp

as diffusional broadening is effectively suppressed by electromigrational (isotachophoretic) sharpening. After leaving the stack, *i.e.*, at times $t > t_{X,e}$, normal diffusional broadening of zone X proceeds. The total variance of this zone at the detection time t_r is then

$$\sigma_{X,r}^2 = \sigma_{X,e}^2 + 2D_X (t_{X,r} - t_{X,e}) \tag{25}$$

where $\sigma_{X,e}^2$ is the zone variance at time $t_{X,e}$. Substitution from eqn. 24 and rearrangement give

$$\sigma_{X,r}^2 = 2D_X \cdot \frac{x_r}{v_{X,1}} + \sigma_{X,e}^2 - 2D_X\, t_{X,e} \cdot \frac{u_X}{u_A} \tag{26}$$

This equation consists of three terms of which the first, $2D_X x_r / v_{X,1}$, expresses the variance the zone would have when undergoing normal zone electrophoresis. The variance in the present instance is lower because the diffusional peak broadening does not proceed as long; this is expressed by the third term. On the other hand, some variance is contributed by the concentration peak not being infinitely sharp when migrating out of the stack (second term in eqn. 26). We may expect that $\sigma_{X,e}^2$ is much smaller than $\sigma_{X,r}^2$, *i.e.*, that the minor sample component undergoes efficient concentrating/stacking at the rear boundary of the zone of the major sample component. In such a case the resulting peak variance is smaller than in normal zone electrophoresis. Eqn. 26 also implies one important fact, *viz.*, owing to the mentioned stacking effect, the resulting variance of a sample zone is independent of the injection conditions.

Separation and resolution of a pair of minor sample components

The above considerations may now be used to describe the case that is of analytical interest, *viz.*, the separation and resolution of a pair of minor sample components, say substances X and Y. If we assume that the separation from the major component (component A) and the zone migration of each minor sample component proceed independently of each other, we can directly use the results in the previous section.

The resulting distance of two separated sample peaks can be expressed as the difference in detection times; from eqn. 24 we obtain directly

$$\Delta t_{X,Y,r} = \frac{x_r}{v_{X,1}} \cdot p_{X,Y} - t_d \cdot \frac{(u_A - u_B)^2}{u_A} \cdot$$

$$\frac{u_X - u_Y}{(u_A - u_X)(u_A - u_Y)} \quad (27)$$

where $p_{X,Y} = (u_X - u_Y)/u_Y$ is the selectivity between X and Y. The first term corresponds to the case of normal zone electrophoresis. The second term represents the decrease in the detection times difference of the present case when compared with simple zone electrophoresis; the reason is the same as for the increase in detection time in eqn. 24.

The time-based variance of the peak of component i passing through the detector may be approximated by

$$^t\sigma_{i,r} = \sigma_{i,r}/v_{i,1} \quad (28)$$

The resolution is thus

$$R_{X,Y} = \frac{\Delta t_{X,Y,r}}{2 \left(^t\sigma_{X,r} + {}^t\sigma_{Y,r} \right)} \quad (29)$$

When compared with normal zone electrophoresis, the resolution here is decreased by the nominator and increased by the denominator (see the comments on eqns. 27 and 26, respectively).

EXPERIMENTAL

Computer simulations were performed using the model by Bier et al. [18] and Mosher et al. [10] in the form of a PC-adapted software package. The software was run on a Mandax AT 286 computer (Panatronic, Zürich, Switzerland) featuring a mathematical coprocessor, a 40 Mbyte hard disk and 1 Mbyte of RAM memory. The simulation results were imported into SigmaPlot Scientific Graphing Software version 4.01 (Jandel Scientific, Corte Madera, CA, USA) and the plots were printed on an HP Laserjet IIIP printer (Hewlett-Packard, Widen, Switzerland).

For all simulations, the same model system was taken with the ionic mobility values $u_A = 8 \cdot 10^{-8}$ m^2 V^{-1} s^{-1}, $u_B = 3 \cdot 10^{-8}$ m^2 V^{-1} s^{-1} and $u_{RH} = 4 \cdot 10^{-8}$ m^2 V^{-1} s^{-1}. The dissociation constant of the counter-species was taken as p$K_a = 6$. The concentration of the background electrolyte of like charge was $c_{B,1} = 0.1$ M and the concentration of the major sample ion in the sample zone was

$c_{A,3} = 0.1$ M; the concentrations of all minor sample components in the sample zone were $1 \cdot 10^{-4}$ M and the concentration of the counter component was 0.2 M. The electric current density was kept constant at 2000 A m^{-2} in all simulations.

RESULTS AND DISCUSSION

To illustrate the theoretical considerations presented, computer simulations of model systems were performed. Although the conclusions in the Theoretical section are valid for the separations of both anions and cations, all the simulations performed
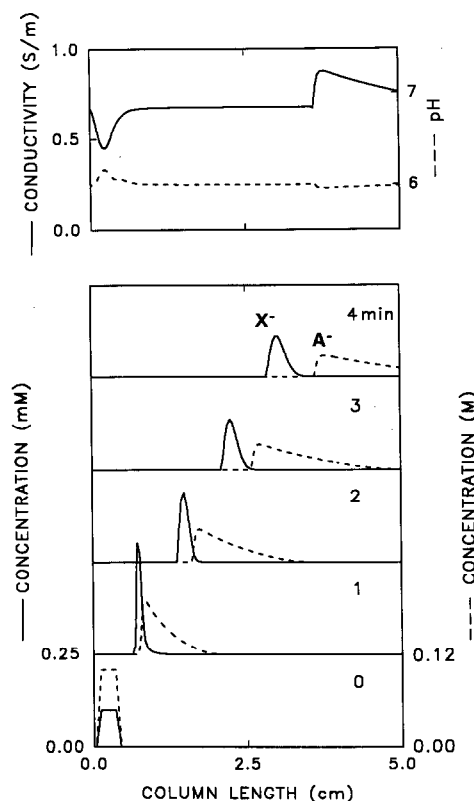

Fig. 3. Computer simulation of zone electrophoretic migration of a minor amount of strong anion X$^-$ ($u_X = 45 \cdot 10^{-9}$ m^2 V^{-1} s^{-2}) in the presence of a major amount of a strong and fast anion A$^-$. The lower panel shows the simulated concentration profiles of both components after 0, 1, 2, 3 and 4 min of electrophoresis time (see the numbers on the right; the concentration scale of each following time point is shifted upwards using an offset of 0.25 mM). The upper panel shows pH and conductivity profiles along the column for the last time point (4 min). Simulation was performed for an 8-cm long column with 200 segments; the initial sample pulse length was 0.32 cm.

are related to anionic separations. Fig. 3 shows typical simulation data of a simple model system with the major sample anion and one minor sample component. The depicted evolution of the concentration profiles clearly shows both the concentration and stacking of the minor component at the rear boundary of the zone of the major component (see profile at 1-min electrophoresis time) and the subsequent migration of the minor component zone out of the stack and its gradual broadening. For this example, the time of the beginning of destacking calculated from eqn. 19 is 1.3 min. This result compares favourably with that obtained by computer simulation. The pH and conductivity data presented in the top panel of Fig. 3 (last time point only) depict that the major component strongly influences the local conductivity and pH. This is not the case for the minor component. These findings are in complete agreement with previous computer simulations [10,19]. Nevertheless, the pH deviation does not exceed ca. 0.2 units, showing that the presumption made in the Theoretical section were justified.

Fig. 4 makes use of a similar simulation run with one minor sample component and gives details on the process of zone broadening. After sharpening (first 30 s) the zone variance is very low and remains almost constant. It starts to increase shortly before the electrophoresis time approaches the value of $t_{X,e}$
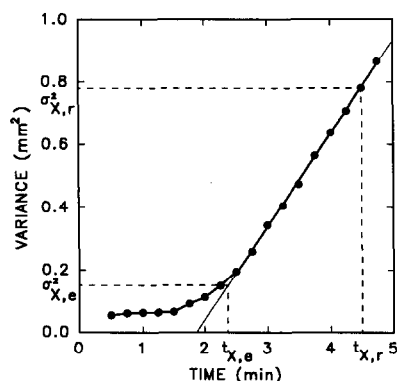
(2.4 min, calculated from eqn. 19). As expected, the zone variance shows a perfect linear dependence on time at times higher than 2.4 min (see eqn. 25 and the marked values of $\sigma^2_{X,r}$, $\sigma^2_{X,e}$, $t_{X,r}$ and $t_{X,e}$).

In order to obtain a better insight into the discussed type of systems, some numerical calculations were performed for the given model system and for a pair of minor sample components. For a 0.3-cm long sample pulse with the concentration of the major component being $c_{A,3} = 100$ mol m^{-3}, we obtain the parameters of the system, viz., the time when the sample completely leaves the sampling compartment $t_0 = 22.5$ s (eqn. 4), the isotachophoretic velocity of the self-sharpening boundary stack, $v_{1-2} = 0.86 \cdot 10^{-4}$ m s^{-1} (eqn. 5), the velocities of the front and rear edges of the transient zone 21, $v_{A,1} = 2.29 \cdot 10^{-4}$ m s^{-1} (eqn. 6) and $v_{B,2} = 0.32 \cdot 10^{-4}$ m s^{-1} (eqn. 6), respectively, and the specific conductivity of the background electrolyte, $\kappa_1 = 0.7$ S m^{-1} (see eqn. 3). Note the great difference between the velocities of both edges of

Fig. 4. Simulated dependence of the variance of the concentration profile of zone X ($u_X = 55 \cdot 10^{-9}$ m^2 V^{-1} s^{-2}) on time. Simulation was performed for a 10-cm long column with 400 segments; the initial sample pulse length was 0.3 cm. The variance was evaluated from the peak width at half-height (W) of the plotted simulation results using the equation $\sigma^2 = W^2/5.545$. For explanation, see text.

TABLE I

NUMERICAL VALUES OF ZONE PARAMETERS OF SEPARATION OF A PAIR OF MINOR SAMPLE COMPONENTS X$^-$ AND Y$^-$ ($u_X = 45 \cdot 10^{-9}$ m^2 V^{-1} s^{-2}, $u_Y = 40 \cdot 10^{-9}$ m^2 V^{-1} s^{-2}) AND THEIR DEPENDENCE ON THE CONCENTRATION OF THE MAJOR SAMPLE COMPONENT

The sample pulse length was 0.3 cm and the detector was positioned at $x = 10$ cm. The current density was 2000 A m^{-1}.

Parameter	$c_{A,3}$ (mol m^{-3})			
	0	50	100	200
κ_3 (S m^{-1})	0.00165	0.6	1.2	2.4
t_d (eqn. 12) (s)		18.1	36.2	72.3
$x_{X,e}$ (eqn. 21) (cm)		0.27	0.53	1.07
$x_{Y,e}$ (eqn. 21) (cm)		0.16	0.32	0.65
$t_{X,e}$ (eqn. 19) (s)		36.9	73.8	147.6
$t_{Y,e}$ (eqn. 19) (s)		28.3	56.5	113.0
$t_{X,r}$ (eqn. 24) (s)	778	794	810	842
$t_{Y,r}$ (eqn. 24) (s)	875	889	903	932
$\Delta t_{X,Y,r}$ (eqn. 27) (s)	97	95	93	90
$\sigma^2_{X,r}$ (eqn. 26)^a (mm^2)	1.70	1.71	1.67	1.59
$\sigma^2_{Y,r}$ (eqn. 26)^a (mm^2)	1.70	1.73	1.70	1.65
$^t\sigma^2_{X,r}$ (eqn. 28) (s)	10.14	10.17	10.05	9.81
$^t\sigma^2_{Y,r}$ (eqn. 28) (s)	11.44	11.51	11.41	11.24
$R_{X,Y}$ (eqn. 29)	2.25	2.19	2.17	2.14

^{a} $D_i = RTu_i/F$; $\sigma^2_{X,e} = \sigma^2_{Y,e} = 0.05$ mm^2.

zone 21, which indicates the fast growing and flattening of the concentration profile of A^-. Further numerical data including those calculated for the minor sample components X^- and Y^- ($u_X = 45 \cdot 10^{-9}$ m^2 V^{-1} s^{-2}, $u_Y = 40 \cdot 10^{-9}$ m^2 V^{-1} s^{-2}) are given in Table I. As can be seen, the time points of leaving the stack, $t_{i,e}$, are low for both components when compared with the final detection times $t_{i,r}$ for the present length of the sample pulse. Nevertheless, they differ substantially (see the dependence on mobility, u_X or u_Y, in eqn. 19). For $t_{i,e} > t_{i,r}$, the sample zone would pass through the detector still in the stack. However, only very high concentrations of A^- in the sample would lead to such an increase in the $t_{i,e}$ values, e.g., for X^- in Table I, the critical value of $c_{A,3}$ is as high as 1.88 M.

Interesting conclusions may be drawn from Table I by comparing the data for various concentrations of the major sample anion and especially for the case with $c_{A,3} = 0$ (the sample solution contains only the minor sample components). It is seen that the presence of A^- in the sample substantially changes (increases) the detection times of both components; this is given by the dependence of $t_{i,e}$ on t_d (see eqn. 19). The difference in the detection times of X^- and Y^-, however, remains nearly constant, decreasing only slightly with increasing $c_{A,3}$. As far as zone broadening is concerned, Table I shows that for the case presented there is no substantial difference in zone variance between the case with and without A^- in the sample. The final resolution decreases slightly with increasing concentration of the major sample component.

It can be concluded from the data presented in Table I that the systems with sample self-stacking provide a similar separation power for minor sample components compared with the samples containing only these minor sample components. The analysis times are slightly increased in the presence of a major compound of like charge. This is illustrated with the
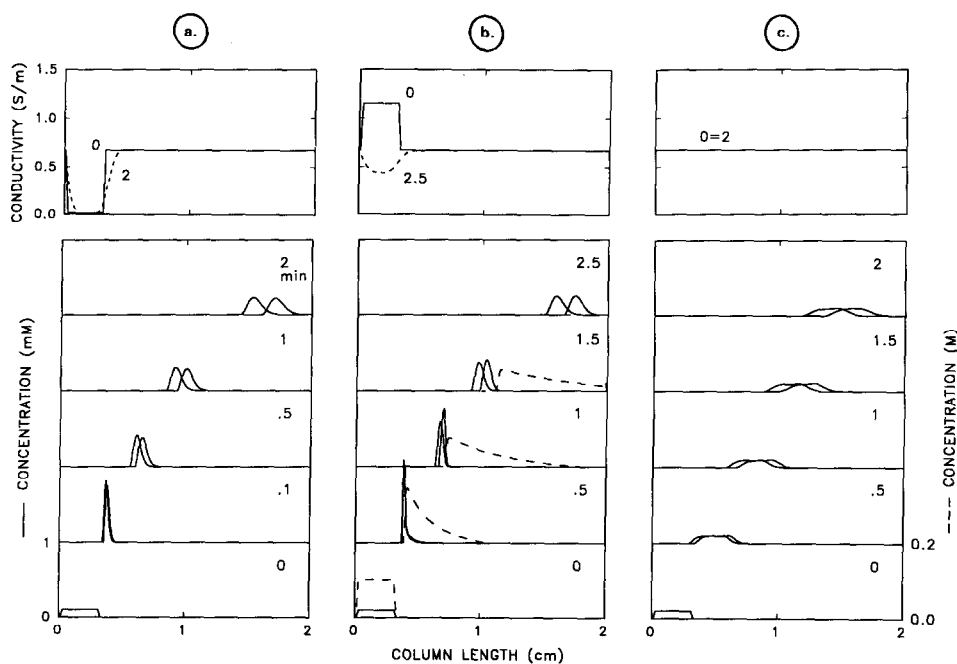

Fig. 5. Computer-simulated dynamics of the concentration profiles during the separation of two strong anions X^- and Y^- ($u_X = 40 \cdot 10^{-9}$ m^2 V^{-1} s^{-2}, $u_Y = 35 \cdot 10^{-9}$ m^2 V^{-1} s^{-2}). The sample contained X^- and Y^- ($1 \cdot 10^{-4}$ M each) with (a) addition of a 0.002 M concentration of the background electrolyte anion B^-, (b) addition of a 0.1 M concentration of anion A^- (the profile of A^- is shown by the dashed line) and (c) addition of a 0.1 M concentration of the background electrolyte anion B^-. The electrophoresis time in minutes of each profile is shown by the numbers on the right. The three upper panels show the conductivity profiles along the separation column at the first (solid line) and last (broken line) time point of each simulation; the numbers indicate the respective electrophoresis time in minutes. Simulation was performed for a 2-cm long column with 200 segments; the initial sample pulse length was 0.3 cm.

simulation data depicted in Fig. 5. Fig. 5a shows the situation with the sample solution containing the two minor components accompanied by a minute concentration of background electrolyte. Here, the sample stacking effect applies (see Introduction) owing to the very low conductivity of the sample solution (see top panel of Fig. 5a). Effective sharpening of the sample zones is seen at the beginning of the analysis. Fig. 5b illustrates the case where the sample shows the self-stacking effect produced by the presence of A^-. Although the conductivity of the sample solution is even higher than that of the BGE (see top panel of Fig. 5b), effective sharpening of both zones of the separated components is seen at the rear of the zone of the major component. Comparison of Fig. 5a and b reveals that the sample self-stacking mechanism has approximately the same effect as normal sample stacking. For comparison, Fig. 5c shows the case when the sample is dissolved in the background electrolyte. The conductivities of the sample solution and of the BGE are the same and there is no

mechanism to sharpen the zones. Flat zone patterns and poor resolution are the result.

Fig. 6 illustrates the self-sharpening effect in multi-component samples by showing the simulation result for a sample with four minor substances and one major component of like charge. As can be seen, the very narrow zone stack spreads gradually into four individual peaks. The time point at which the sample components begin to migrate out of stack is given by the mobility of the respective substance; for the anions with mobilities $35 \cdot 10^{-9}$, $45 \cdot 10^{-9}$, $55 \cdot 10^{-9}$ and $65 \cdot 10^{-9} \text{ m}^2 \text{ V}^{-1} \text{ s}^{-2}$, eqn. 19 provides destacking times of 0.7, 1.2, 2.4 and 6.7 min, respectively. At $t = 5$ min, for example, three of the four zones are already destacked and broadening; only the fastest component with the highest mobility remains in the stack, as is demonstrated by its narrower shape.

CONCLUSION

The sample self-stacking effect belongs to the sampling techniques which provide electromigrative concentration of minor sample components into narrow zones. The concentration power of this technique is about the same as with, e.g., normal sample stacking, but the application range is different. The sample self-stacking applies to minor components in samples containing a bulk amount of a high-mobility ion of like charge. A necessary condition is that the mobility of the background co-ion is lower than the mobilities of all the sample components so that it can act as a terminator of the stacking process. The process of sample self-stacking can be described by simple relationships describing the timing of the particular steps of the process, viz., readjustment of the sample concentrations to the parameters of the background electrolyte, isotachophoretic stacking of the minor sample components at the rear boundary of the major component zone and destacking followed by normal zone electrophoretic migration. The numerical values compare well with data obtained by computer simulation. Interestingly, the final resolution does not show a pronounced dependence on either electric current density or initial concentration of the major component in the sample. This concentration, however, significantly affects the conductivity of the sample solution and thus the Joule heating in the
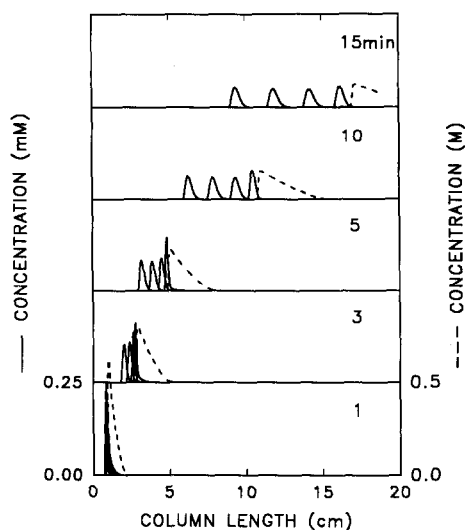

Fig. 6. Computer-simulated dynamics of the zone electrophoretic separation of four strong anions with mobilities $35 \cdot 10^{-9}$, $45 \cdot 10^{-9}$, $55 \cdot 10^{-9}$ and $65 \cdot 10^{-9} \text{ m}^2 \text{ V}^{-1} \text{ s}^{-2}$ in the presence of a major amount of a strong and fast anion A^-. The initial concentration of all minor sample components was $1 \cdot 10^{-4} M$. The concentration profiles of all four components and of anion A^- (dashed line) are shown at 1, 3, 5, 10 and 15 min of electrophoresis time (see the numbers on the right). Simulation was performed for a 20-cm long column with 400 segments; the initial sample pulse length was 0.3 cm.

sampling compartment. Addition of a fast anion to dilute solutions of thermolabile samples may therefore prevent their thermal degradation, which is a real problem when using normal sample stacking [20]. The concentration of the major component in the sample significantly affects the elution times of the individual minor components. As these differences represent typically tens of percent, qualitative evaluations of electropherograms must be performed with great care in all instances where sample self-stacking may apply. The equations presented may be easily modified to describe cationic separations and systems with electroosmotic flow.

ACKNOWLEDGEMENT

REFERENCES

1 F. E. P. Mikkers, F. M. Everaerts and Th. P. E. M. Verheggen, *J. Chromatogr.*, 169 (1979) 11.
2 S. E. Moring, J. C. Colburn, P. D. Grossman and H. H. Lauer, *LC · GC*, 8 (1989) 34.
3 R. L. Chien and D. S. Burgi, *J. Chromatogr.*, 559 (1991) 141.
4 P. Jandik and W. R. Jones, *J. Chromatogr.*, 546 (1991) 431.
5 D. Kaniansky and J. Marák, *J. Chromatogr.*, 498 (1990) 191.
6 V. Dolník, K. A. Cobb and M. Novotny, *J. Microcol. Sep.*, 2 (1990) 127.
7 F. Foret, V. Šustáček and P. Boček, *J. Microcol. Sep.*, 2 (1990) 229.
8 F. Foret, E. Szoko and B. L. Karger, *J. Chromatogr.*, 608 (1992) 3.
9 R. A. Mosher and W. Thormann, *Pittsburgh Conference and Exposition, New Orleans, February 22–26, 1988*, Abstract No. 646.
10 R. A. Mosher, D. A. Saville and W. Thormann, *The Dynamics of Electrophoresis*, VCH, Weinheim, 1992.
11 Th. P. E. M. Verheggen, A. C. Schoots and F. M. Everaerts, *J. Chromatogr.*, 503 (1990) 245.
12 A. C. Schoots, Th. P. E. M. Verheggen, P. M. J. M. De Vries and F. M. Everaerts, *Clin. Chem.*, 36 (1990) 435.
13 J. L. Beckers and F. M. Everaerts, *J. Chromatogr.*, 508 (1990) 19.
14 P. Boček, M. Deml, P. Gebauer and V. Dolník, *Analytical Isotachophoresis*, VCH, Weinheim, 1988.
15 H. Weber, *Die Partiellen Differential-Gleichungen der Mathematik und Physik*, Vol. I, Friedrich Vieweg u. Sohn, Braunschweig, 1910, p. 503.
16 P. Gebauer, M. Deml, J. Pospíchal and P. Boček, *Electrophoresis*, 11 (1990) 724.
17 L. M. Hjelmeland and A. Chrambach, *Electrophoresis*, 3 (1982) 9.
18 M. Bier, O. A. Palusinski, R. A. Mosher and D. A. Saville, *Science (Washington, D.C.)*, 219 (1983) 1281.
19 W. Thormann, J. P. Michaud and R. A. Mosher, in M. J. Dunn (Editor), *Electrophoresis '86*, VCH, Weinheim, 1986, p. 267.
20 A. Vinther and H. Soeberg, *J. Chromatogr.*, 559 (1991) 27.